CHAPTER 5

Effect of 140 Mev Ag+11 ion irradiation on some commercially available composites

This chapter deals with the electrical, optical, structural characteristics of 140 Mev Ag^{+11} ions irradiated PP+TiO_2, PP+GF and HDPE+CB composites at different ion fluences by different characterization techniques viz dielectric study, UV-spectroscopy, X-ray diffraction analysis and surface morphology of the composites.

5.0 Introduction

High energy ion beam irradiation tends to damage polymers significantly by electronic excitation and ionization processer. It may result in the creation of latent tracks in the polymers and can also cause formation of free radicals, chain scission, intermolecular cross-linking, creation of double/triple bonds, unsaturated bonds and loss of volatile fragments [1,2]. The nature of the defects and the relative radiative sensitivity of different polymers depend on the properties such as the composition and molecular weight, mass and energy of the impinging ion and also on the environmental conditions during irradiation. The use of ion beam irradiation is getting high impetus as chemical composition and the related physical properties of the polymers can be modified in a controlled way by controlling parameters like the energy and ion fluence.

We have studied the effect of high energy ion beam irradiation on the following polymer composites:

5.1 Polypropylene/TiO2 composites [3]

5.2 Polypropylene/ Glass fiber composite [4]

5.3 High density polyethylene/carbon black composites [5]

5.1 Effect of 140 MeV Ag^{11+} ion irradiation on polypropylene/TiO_2 composites

5.1.1 Introduction

The homopolymer polypropylene (PP), a plastic material used as packaging and for medical products, must be subjected to a form of sterilization. PP has the advantage of being nontoxic and inert to liquids and drugs. It is also used as capacitor dielectric because of its very low dielectric loss and excellent dielectric strength [6]. The properties of PP have been discussed in Chapter-2. Titanium dioxide or titania (TiO_2)

is a harmless white material widely used in photo electrochemical solar energy conversion and environmental photo catalysis (treatment of polluted water and air) including self cleaning and anti fogging surfaces [7, 8]. It is also commonly used as a high refractive index material in optical filter applications and sensors [9, 10]. Nanostructured TiO2 is used in solar cell research and displays [11].TiO_2 thin films are valued for their good durability, high dielectric constant, high refractive index, excellent transparency in the visible range and biocompatibility. In polymer light emitting diode devices, mixing TiO_2 nanoparticles into poly[2-methoxy-5-(2'-ethyl-hexyloxy)-para-phenlenevinylene] MEH-PPV results in increased current densities, radiances and power efficiencies [12,13].

The irradiation effects in inorganic materials are known to be manifested as change in the physical properties such as refractive index, magnetization and hardness [14]. The fundamental processes associated with these changes are defect formation through electronic and nuclear interactions of radiation and the subsequent chemical interaction between the defects and elements in the materials. Study of radiation induced defects in inorganic compounds is important for their role in device fabrication [15].

The aim of this work is to study the effect of SHI irradiation on the electrical, structural, optical properties and surface morphology of PP/TiO_2 composites. Properties and target details of composites have been discussed in Chapter-2. All pallets were irradiated with 140 MeV Ag11+ ions at the fluences of $1x10^{11}$ and $5x10^{12}$ ions/cm^2 using Pelletron accelerator at Inter University Accelerator Centre (IUAC), New Delhi.

5. 1.2 Results and discussion

5.1.2.1 UV- Vis. spectrometry

It has been observed that there are sharp changes in surface color of irradiated samples and it became brownish at a fluence of $5x10^{12}$ ions/cm^2. The absorption of the light energy by the composites in the ultraviolet and visible regions involves promotions of electrons in σ, π and n-orbital from ground state to higher energy state [16]. Figure 5.1(a) shows UV- visible absorption spectra of unirradiated and silver ion irradiated ($5x10^{12}$ ions/cm^2) PP+TiO_2 composite samples in the wavelength range 200-900 nm.

It clearly indicates a peak at 384 nm and after the irradiation, the peak was shifted to 404 nm. Such a shift in absorption peak towards higher wavelength indicates a decrease in energy band gap of the composite upon irradiation due to breakage of bonds and formation free radicals, unsaturation etc. and hence an increase in conductivity is also observed [17, 18].

The optical band edge can be correlated with the optical band gap E_g by Tauc's expression [19]

$$\omega^2 \varepsilon_2 (\lambda) = (h\omega - E_g)^2$$

Where ε_2 (λ) is the imaginary part of the complex refractive index, that is optical absorbance and λ is the wavelength.

For the determination of direct and indirect band gaps, $(\alpha h\nu)^2$ and $(\alpha h\nu)^{1/2}$ were plotted as a function of photon energy ($h\nu$) respectively [20] taking into account the linear portion of the fundamental absorption edge of the UV-visible spectra as shown in figures 5. 1(b) and 5.1(c) for pristine and irradiated PP+TiO_2 composites respectively. The intercept of the best fit line on $h\nu$ axis revealed the direct and indirect band gaps for pristine and irradiated PP+TiO_2 composites. These results are presented in Table 5.1.

The regression coefficient 'R' was found to be greater than 0.95 from the fitted line and was used to determine the direct and indirect band gaps. It reveals the simultaneous existence of direct and indirect band gaps in PP+TiO_2 composites with decreasing in its value upon irradiation. The decrease in band gap is attributed to the scissioning of polymer chain due to irradiation and as a result creation of free radicals, unsaturation etc and thus have a capability of increasing the conductivity of the composites. Furthermore, the value of indirect band gap was found to be lower than that of direct band gap. Simultaneous existence of direct and indirect band gaps were also reported in some other materials [20,21]. To the best of our knowledge simultaneous existence of direct and indirect band gaps in polypropylene/TiO_2 composite has not yet been reported so far.

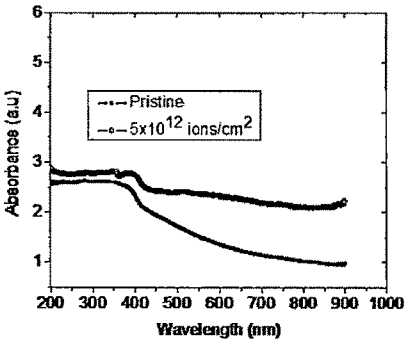

(a)

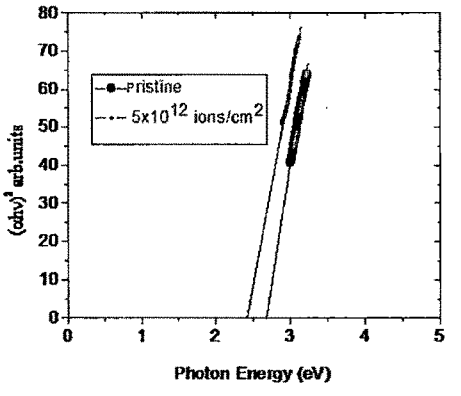

(b)

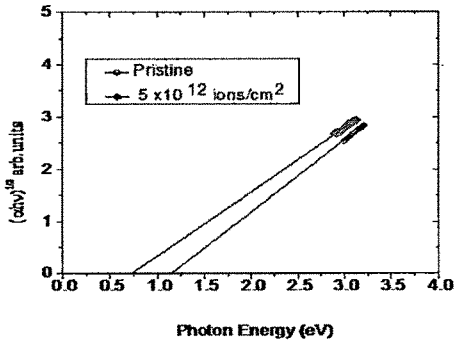

(c)

Fig. 5.1 (a) UV-Visible absorption spectra of pristine and irradiated PP+TiO_2 polymer composites. (b) Plot of direct band gap (eV) for pristine and irradiated PP+TiO_2 polymer composites. (c) Plot of indirect band gap (eV) for pristine and irradiated PP+TiO_2 polymer composites.

Table. 5.1

Table 1 Direct and indirect band gap values for pristine and irradiated PP+TiO_2 composites.

Samples	Direct band gap (eV)	Regression coefficient 'R'	Indirect band gap (eV)	Regression coefficient 'R'
Pristine	2.62	0.99	1.18	0.99
Irradiated	2.42	0.99	0.70	0.99

5.1.2.2 X-ray diffraction analysis

The diffraction patterns of pristine and irradiated polypropylene/TiO_2 composites are shown in figure 5.2. The six peaks were recorded at 2θ =12.49, 13.82, 19.09, 21.21, 28.90, and 42.94. It clearly indicates that the polypropylene/TiO_2 composite is crystalline in nature. It was observed from the diffraction pattern of irradiated sample that there is an increase in the peak intensities and decrease in the full width at half maximum (FWHM) corresponding to all observed peaks. The decrease in FWHM and increase in peak intensity is generally associated with increase in crystallinity of the sample due to ion beam irradiation. Degree of crystallinity (K) was calculated using formula

K = (Area under diffraction peak/ Total area under diffractogram) x 100%

Degree of average crystallanity was found 5.47% and 6.35% for pristine and irradiated samples respectively. The degree of crystallinity has increased significantly due to irradiation, which could be attributed to alignment of polymer chain by chain folding / cross linking of polymer chains or due to the formation of single or multiple helices along their length [22]. The average crystallite size (t) for pristine and irradiated samples was calculated using Scherrer's formula [23]

$t = 0.9\,\lambda / (B\,\mathrm{Cos}\theta)$

Where λ =1.5418 A^0 is the wavelength of the Cu K_α X-ray radiation used to record powder XRD spectra, *B* is FWHM of the diffraction peak and θ is the Bragg angle. The crystallite size was calculated corresponding to six peaks of the pristine and irradiated samples and the results are listed in Table 5.2. The crystallite size was estimated 11.6 nm and 14.1 nm for pristine and irradiated samples respectively.

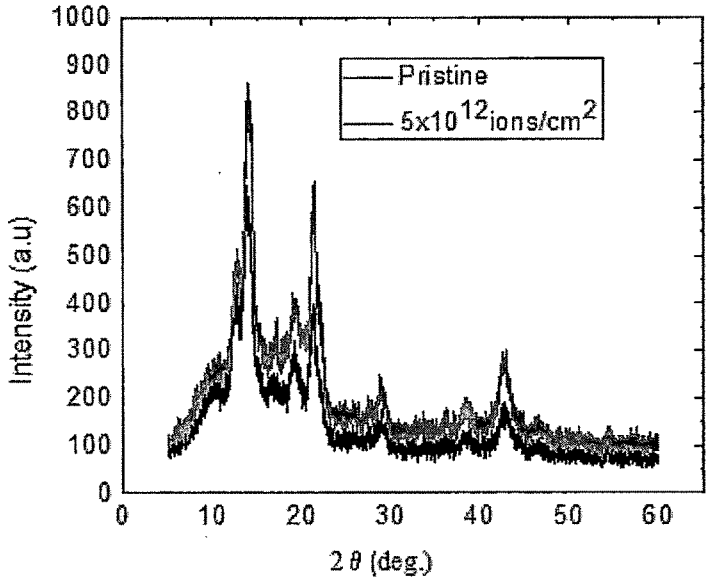

Fig. 5.2 XRD patterns of pristine and irradiated PP+TiO_2 polymer composites at a fluence of $5x10^{12}$ ions/cm^2.

Table.5.2

FWHM, crystallite size and crystallinity of pristine and irradiated polypropylene /TiO2 composites

Pristine				Irradiated (5x 10^{12} ions/cm^2)			
2 theta (deg.)	FWHM (B rad.)	Crystallite Size (nm)	Crystallinity (%)	2 theta (deg.)	FWHM (B rad.)	Crystallite Size (nm)	Crystallinity (%)
12.49	0.7511	11.8	5.60	12.73	0.5000	17.8	5.78
13.82	0.7511	11.8	12.97	13.98	0.5000	17.8	14.40
19.09	0.7254	12.3	3.11	19.21	0.5376	16.7	3.58
21.21	0.7254	12.3	6.89	21.36	0.8061	11.2	8.49
28.90	0.8516	10.7	1.68	28.89	0.8706	10.5	2.21
42.94	0.8735	10.8	2.58	42.94	0.8795	10.8	3.65

Average Crystallite Size =11.6 nm	Average Crystallite Size = 14.1 nm
Average Crystallinity =5.47 %	Average Crystallinity = 6.35 %

5.1.2.3 AC electrical frequency response

(a) Frequency dependence conductivity

AC electrical measurement was performed for pristine and irradiated samples. Figure 5.3 shows the variation of conductivity with log frequency for pristine and irradiated samples. It is observed that the conductivity increases as fluence increases. The increase in conductivity at a given frequency due to irradiation may be attributed to scissioning of polymer chains and as a result increase of free radicals, unsaturation etc. An ac field of sufficiently high frequency may cause a net polarization, which is out of phase with the field. This result in ac conductivity appears at frequency greater than that at which traps are filled or emptied [24].

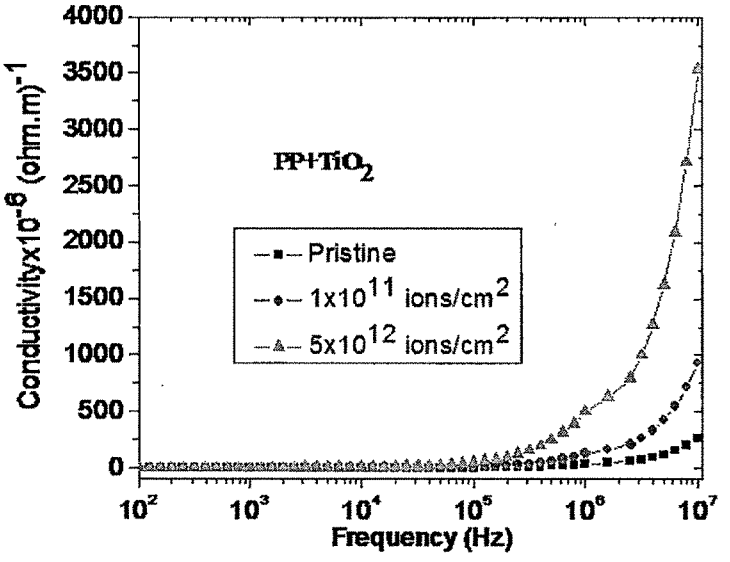

Fig. 5. 3 AC conductivity versus frequency for pristine and irradiated PP+TiO_2 composites at different fluences.

(b) Frequency dependence dielectric constant

Figure 5. 4 shows the plot of dielectric constant versus frequency for pristine and irradiated PP+TiO_2 composite samples. The dielectric constant remains almost constant up to 100 kHz. At these frequencies, the motion of the free charge carriers is constant and so the dielectric constant presumably remains unchanged. As frequency increases further (i.e. beyond 100 kHz), the charge carriers migrate through the dielectric and get trapped against a defect sites and induced an opposite charge in its vicinity. At these frequencies, the polarization of trapped and bound charges can not take place and hence the dielectric constant decreases [25].The dielectric constant obeys the Universal law [24] of dielectric response at higher frequencies (i.e. beyond 100kHz) and given by $\varepsilon \alpha f^{n-1}$, where n is power law exponent and varies between zero to one (0<n<1),and in present study, n=0.38 (for pristine) and 0.44 and 0.91 for irradiated samples at the fluences of $1x10^{11}$ ions/cm^2 and $5x10^{12}$ ions/cm^2 respectively [26]. It is also observed that dielectric constant increases upon irradiation. The increase in dielectric constant may be attributed to the chain scission and as a result the increase in the number of free radicals, unsaturation etc.

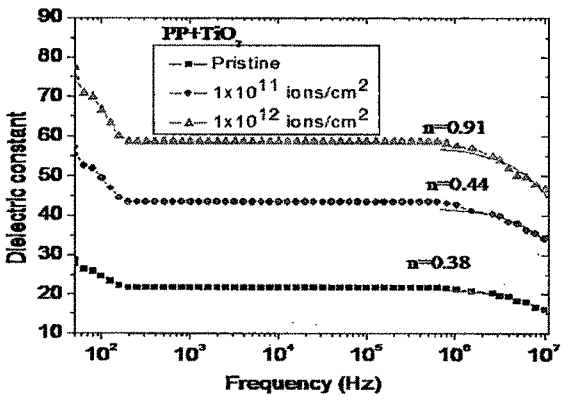

Fig. 5.4. Plot of dielectric constant versus frequency for pristine and irradiated PP+TiO_2 composites at different fluences.

(c) Frequency dependence dielectric loss

Figure 5.5 shows the variation of dielectric loss with frequency for pristine and irradiated PP+TiO_2 composites. The dielectric loss decreases exponentially and then became less dependent on frequency. This is because the induced charges gradually fail to follow the reversing field causing a reduction in the electronic oscillations as frequency increases. It is also noticed that dielectric loss increases moderately with the ion fluence [26].

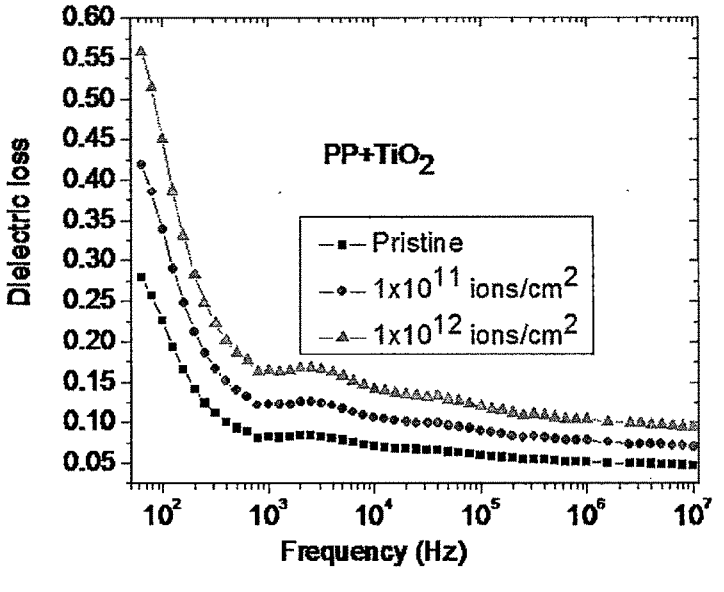

Fig. 5.5. Plot of dielectric loss versus frequency for pristine and irradiated PP+TiO_2 composites at different fluences.

(d) Cole-Cole curve

Figure 5.6 shows the plot of real impedance (z') versus imaginary (z'') components of PP+TiO_2 composites at different fluences. It can be seen from the figure that the curves have certain arc shape that characterizes many semi conducting material. The Cole - Cole constructions yield slightly inclined and distorted semicircles. The geometrical shapes of the complex impedance plane plots indicate that the composite

material is electrically equivalent to RC networks that reduced to pure resistance [27]. In polymer composite samples, there is only one peak in the imaginary impedance and one semicircle in complex plane plot, signifying one relaxation process and also indicating the homogenous materials. It is observed that the diameter of the semicircles decreases as ion fluence increases, which reveals that the conductivity of the composite increases after irradiation. This result is also consistent with the conductivity measurement results (Fig.5.3).

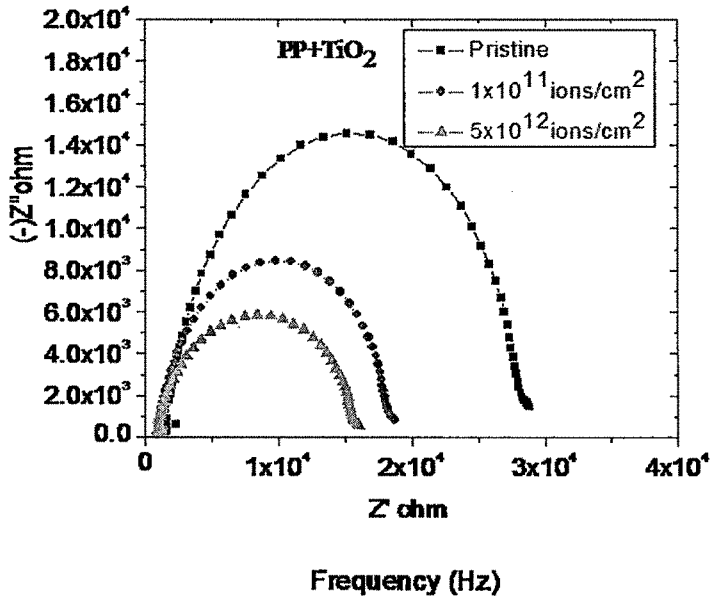

Fig. 5.6 Cole-cole plot for pristine and irradiated PP+TiO_2 composites at different fluences.

5.1.2.4 Surface morphology of the composites

The surface morphology of pristine and irradiated PP+TiO_2 composites was measured by AFM on 5×5 μm^2 area and shown in Figure 5.4.7. Each AFM image was analyzed in terms of surface average roughness (Ra). It is observed that after irradiation the roughness of the surface decreases from 19.6 nm (pristine) to 8.7 nm (irradiated

$5x10^{12}$ ions/cm^2) and the surface became significantly smoother. This relative smoothness is probably due to defect enhanced surface diffusion.

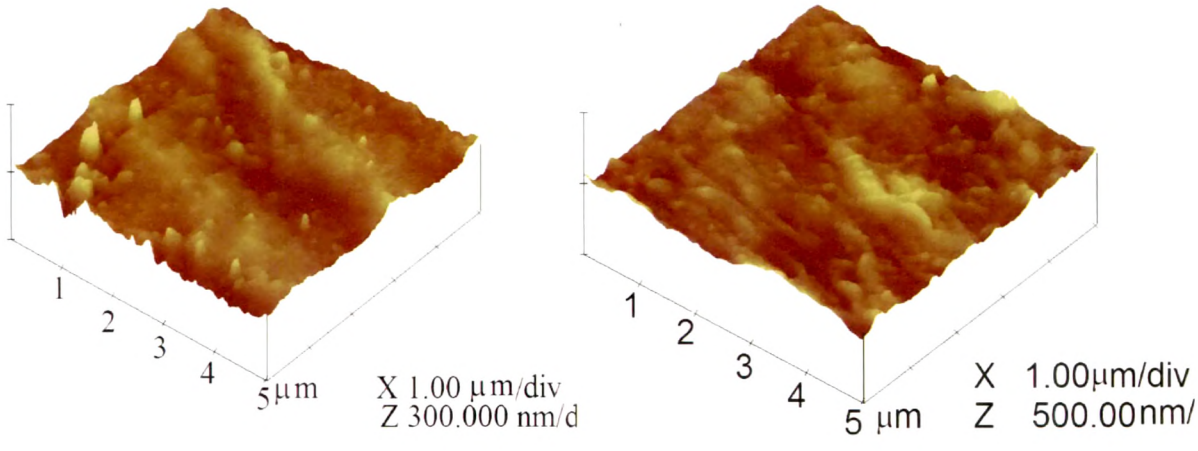

(a) (b)

Fig.5.7. AFM image of PP+TiO_2 Composites (a) pristine PP+TiO_2 (b) PP+TiO_2 irradiated at the fluence of $5x10^{12}$ ions/cm^2.

5.1.2.5 Conclusions

UV-visible spectrophotometric studies of pristine and irradiated polypropylene/titanium oxide composite revealed the coexistence of indirect and direct band gaps. The value of indirect band gap is lower than that of direct band gap in pristine and irradiated polymer composites. From the XRD studies, it was observed that crystallinity of the sample increases due to ion beam irradiation. The dielectric properties of composite are greatly enhanced by ion beam irradiation. Thus irradiation makes the polymer more conductive. This might be attributed to breakage of chemical bonds and resulting in an increase of free radicals, unsaturation etc. It is also observed that dielectric constant obeys Universal law of dielectric response at high frequencies.

The surface roughness of composite decreases upon irradiation as observed from AFM studies.

5.2 Effect of 140 MeV Ag^{+11} irradiation on polypropylene/glass fiber composites

5.2.1 Introduction

Polymer composites are widely used in the aircraft and automotive industries and their high strength to weight ratio makes significant weight reduction possible. Beside these advantages, the polymer materials also offer a good corrosion resistance but the mechanical and electrical properties are not satisfactory. In order to increase these properties glass fibers with high strength can be embedded in polymer matrix [28]. Glass Fiber is most widely used reinforcing material both thermoplastic and thermosetting polymers. It has high tensile strength combined with low extensibility, giving exceptional tensile, compression and impact parameter. It has high temperature resistance and low moisture pick up, giving good dimensional stability and weather resistance. Finally, low moisture absorption makes it possible to produce molding with good electrical properties which do not deteriorate even under adverse weather conditions [29,30].

Interaction of high energy ion beam with polymer results in the formation of gaseous products accompanied by polymer cross linking (i.e. formation of intermolecular bonds), degradation (i.e. scission of bonds in the main polymer chain and side chains) and some other secondary processes [31]. Although both electronic and nuclear energy transfer can induce cross linking as well as scission as would be intuitively expected, experimental evidence suggests that electronic stopping causes more cross linking while nuclear stopping causes more scissions [32,33]. Present work is on polypropylene glass fiber composites and their modifications in electrical, optical, structural properties and surface morphology by swift heavy ion irradiation.

Properties and target details of composites have been discussed in Chapter-2. All pallets were irradiated with 140 MeV Ag^{11+} ions at the fluences of $1x10^{11}$ and $5x10^{12}$ ions/cm^2 using Pelletron accelerator at Inter University Accelerator Centre (IUAC), New Delhi.

5.2.2 Results and Discussion

5.2.2.1 UV-visible spectroscopy

UV- visible is important tools to determine the information about band structure of solids. Insulators/semiconductors are generally classified into two types: (a) direct band gap, and (b) indirect band gap. In the case of direct band gap semiconductors, the top of the valance band and the bottom of the conduction band both lie at same zero crystal momentum (wave vector). If the bottom of the conduction band does not correspond to zero crystal momentum, then it is called indirect band gap semiconductor [34]. We have reported here the direct and indirect band gap for pristine and irradiated polypropylene/glass fiber composites.

Figure 5.8 (a) shows UV- visible absorption spectra of pristine and ion irradiated PP+GF composites in the wavelength range 190-900 nm. It is observed that optical absorption increases upon ion beam irradiation and this absorption shifted from UV to visible region for irradiated polymer composites. The increase in absorption with irradiation may be attributed to the formation of a conjugated system of bonds due to bond cleavage and reconstruction [35, 36]. From the absorption, the band gap of the polymer composite was calculated by linear part of Tauc's expression [19]. For the determination of direct and indirect band gaps, $(\alpha h\nu)^2$ and $(\alpha h\nu)^{1/2}$ were plotted as a function of photon energy ($h\nu$) respectively taking into account the linear portion of the fundamental absorption edge of the UV-visible spectra as shown in Figs. 5.8(b) and 5.8(c) for pristine and irradiated PP+GF composites respectively. The intercept of

the best fit line on hν axis revealed the direct and indirect band gaps for pristine and irradiated PP+GF composites. These results are presented in Table 5.3 The band gap was found to decrease upon ion beam irradiation. It may be due to the higher rate of electronic energy loss by ion beam irradiation which affects the polymer to a greater extent [37, 38].

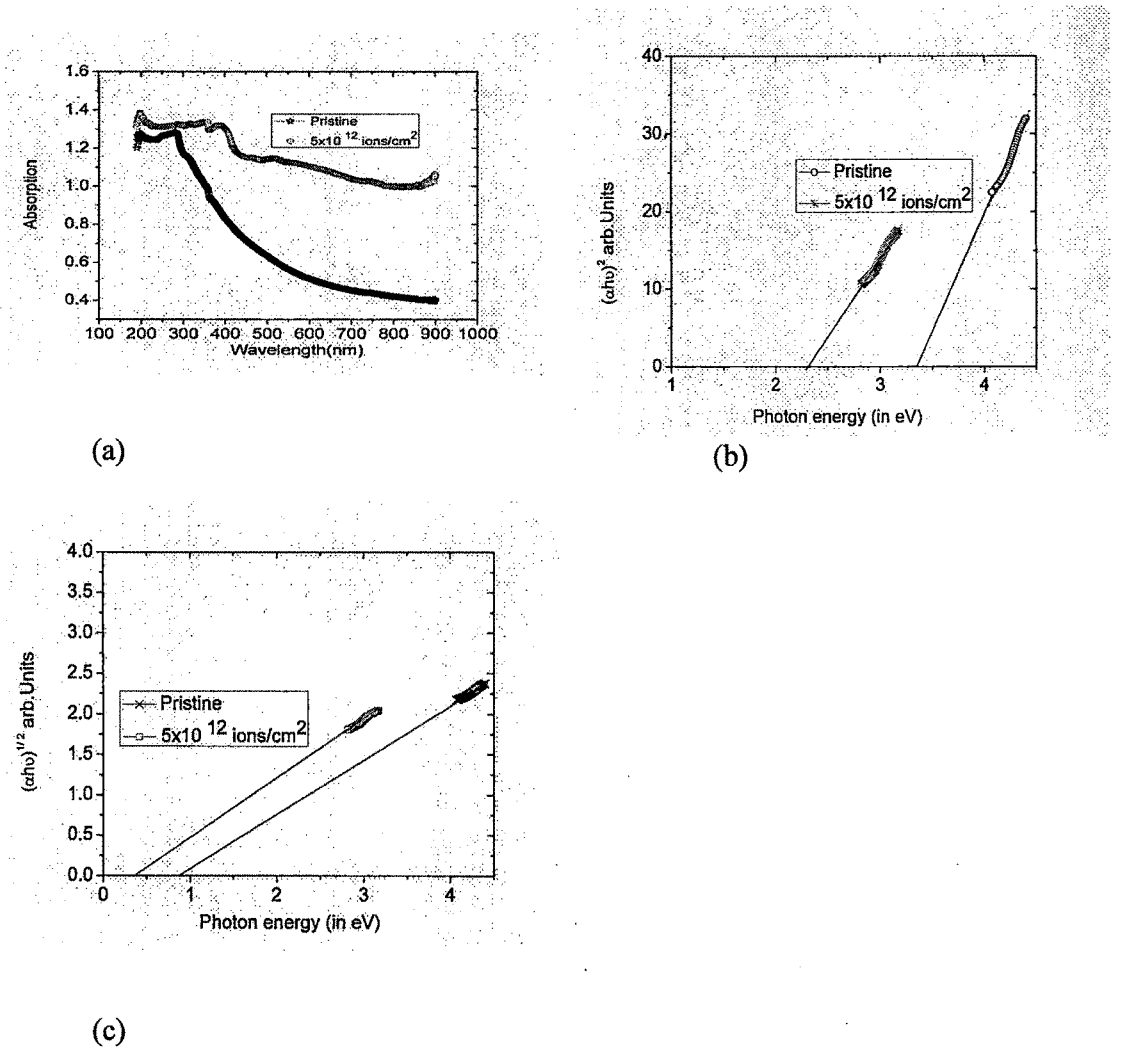

Fig. 5.8 (a) UV-Visible absorption spectra of pristine and irradiated PP+GF polymer composites. (b) Plot of direct band gap (eV) for pristine and irradiated

PP+GF polymer composites. (c) Plot of indirect band gap (eV) for pristine and irradiated PP+GF polymer composites.

Table 5.3 Direct and indirect band gap values for pristine and irradiated PP+GF composites.

Samples	Direct band gap (eV)	Indirect band gap (eV)
Pristine	3.39	0.84
Irradiated	2.33	0.39

5.2.2.2 X ray diffraction analysis

Fig. 5.9 represents the diffraction patterns of the pristine and irradiated samples for the most prominent peak. The peaks are obtained at $2\theta = 12.62^0$, 14.08^0, 16.89^0, 18.62^0, 21.40^0 and 21.80^0. The nature of the peak indicates the semi-crystalline nature of the polymer composites. In both (pristine and irradiated) cases, the peaks obtained approximately at the same position but with different intensity. It is observed that the intensity of XRD pattern decreases with ion beam irradiation and change towards to amorphicity. It reveals that after ion beam irradiation disordering of the material means chain scission in polymer composites, but no significant change in lattice parameter is observed.

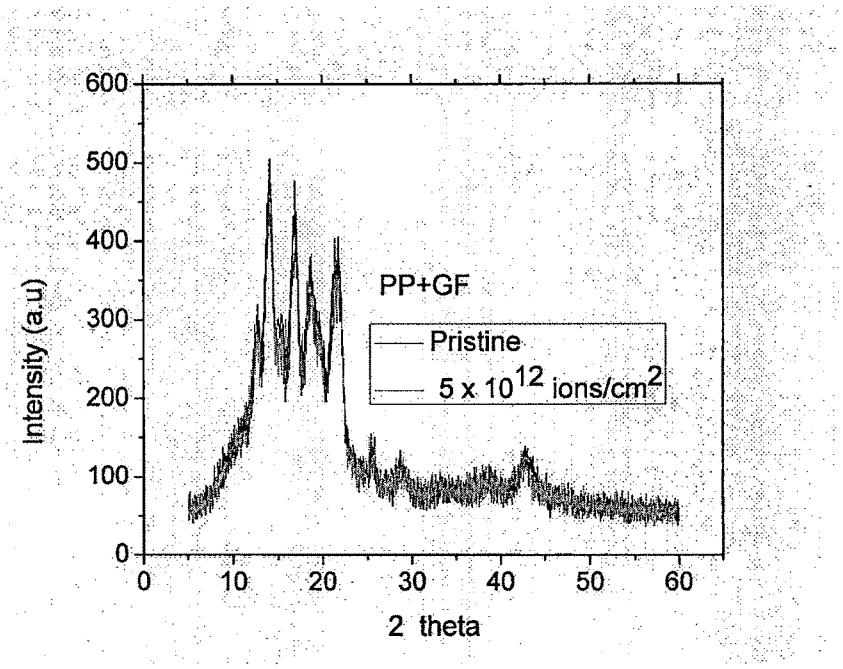

Fig. 5.9 XRD patterns of pristine and irradiated PP+GF composites at a fluence of $5x10^{12}$ions/cm^2.

5.2.2.3 Ac electrical frequency response

(a) Frequency dependence ac conductivity

Figure 5.10 shows the frequency dependent electrical conductivity of pristine and irradiated composites. The conductivity was observed to increase significantly with the fluence, which is attributed to the formation of conjugated double bond, the later one promoting the delocalization of charge carriers, and hence their motion in an external electric field [39].

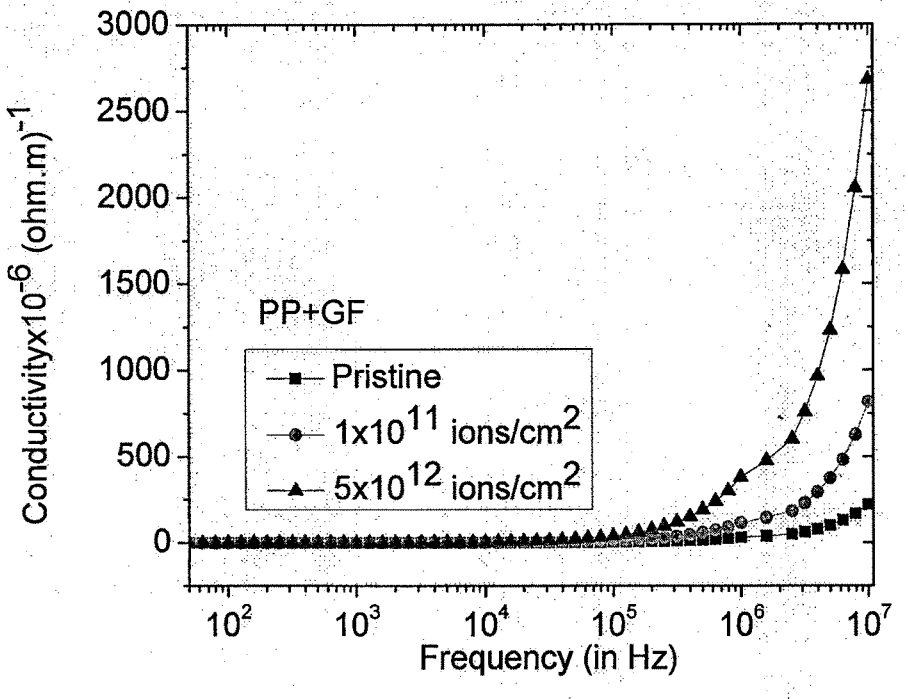

Fig. 5.10 AC conductivity versus frequency for pristine and irradiated PP+GF composites at different fluences.

(a) Frequency dependence dielectric constant

The dielectric constant as a function of frequency from 50 Hz to 10 MHz is shown in Fig.5.11 for pristine and irradiated samples. It is observed that dielectric constant remains almost constant up to 100 kHz, because the motion of charge carriers is almost constant at these frequencies. Beyond this frequency, the dielectric constant decreases. As the frequency increases, the charge carriers migrate through the dielectric and get trapped against the defect sites and they induced an opposite charge in its vicinity, as a result, motion of charge carriers is slowed down and the value of dielectric constant decreases. The decrease in dielectric constant at higher frequency can be explained by Jonscher's power law i.e. $\varepsilon \alpha f^{n-1}$ where $0<n<1$ [24, 25]. The dielectric constant was found to increase by a factor of about 4.0 after SHI irradiation at a fluence of 1x 10 ^{12} ions/cm^2. The drastic increase in dielectric constant due to ion

irradiation may be correlated to the defects created along the ion tracks and structural modifications induced in the surrounding regions. Incident heavy ions get embedded in the polymer or polymer composite loses energy by both the inelastic and elastic collisions. The increase in dielectric constant for irradiated samples may be attributed to the disordering of the material means chain scission in polymer composites and as a result the increase in the number of free radicals, unsaturations etc by the ion beam irradiation. As the fluence increased further the dielectric constant also increases.

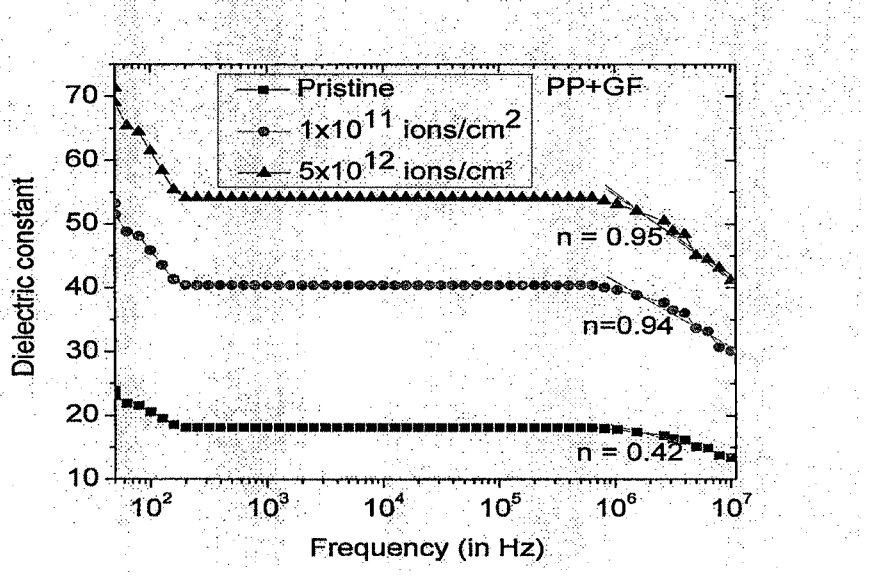

Fig. 5.11 Plot of dielectric constant versus frequency for pristine and irradiated PP+GF composites at different fluencess.

(c) Frequency dependence dielectric loss

Figure 5.12 shows the variation of dielectric loss with frequency for pristine and irradiated PP+GF composites. The dielectric loss decreases exponentially and then became less dependent on frequency. The loss factor (tanδ) shows strong frequency dependence and decreases exponentially as frequency increases. The positive value of tanδ indicates the dominance of inductive behavior [6].

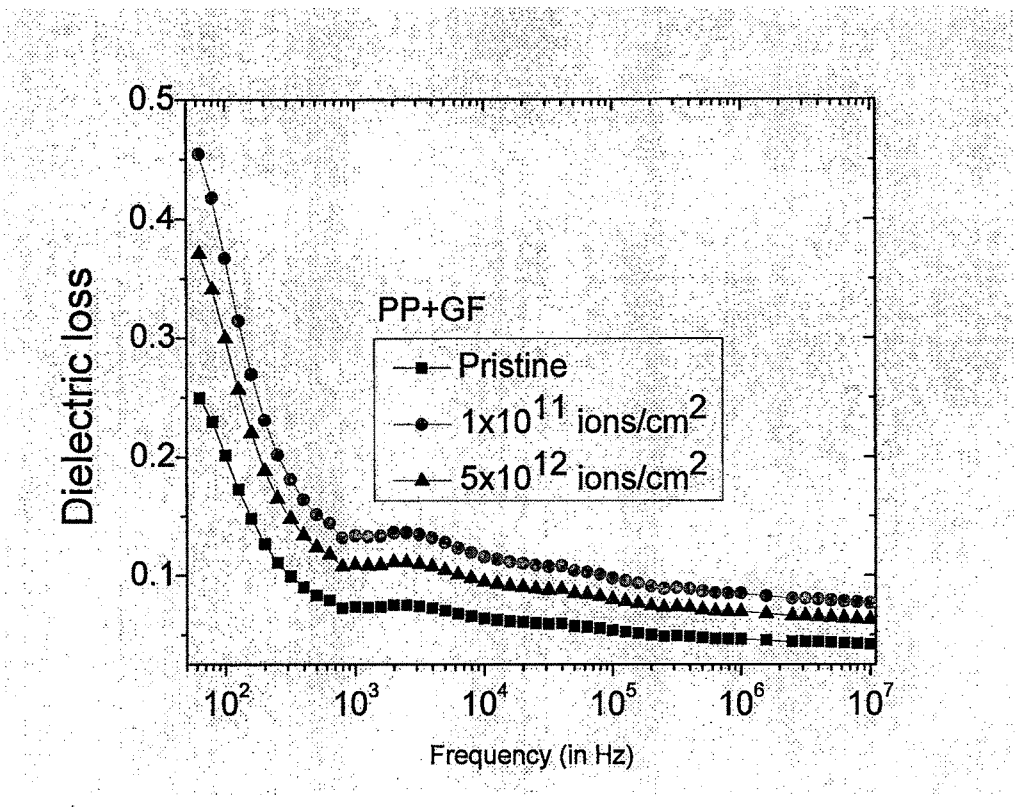

Fig. 5.12 Plot of dielectric loss versus frequency for pristine and irradiated PP+GF composites at different fluences.

(b) Cole- Cole curve

The Cole-Cole plots of pristine and irradiated composites are shown in Fig.5.13. In Cole-Cole presentation, the relaxation mechanisms become evident via the formation of completed or even uncompleted semicircles. The geometrical shapes of the complex impedance plane plots indicate that the composite material is electrically equivalent to RC network that reduces to pure resistance [27]. In our case, there is only one semicircle or arc in complex plane plot for both pristine and irradiated composites, signifying one relaxation process and also indicating the homogenous materials. With increasing ion fluence, the diameter of semicircle decreases, means sample became more conductive, it is also observed by conductivity plot (Fig. 5.13).

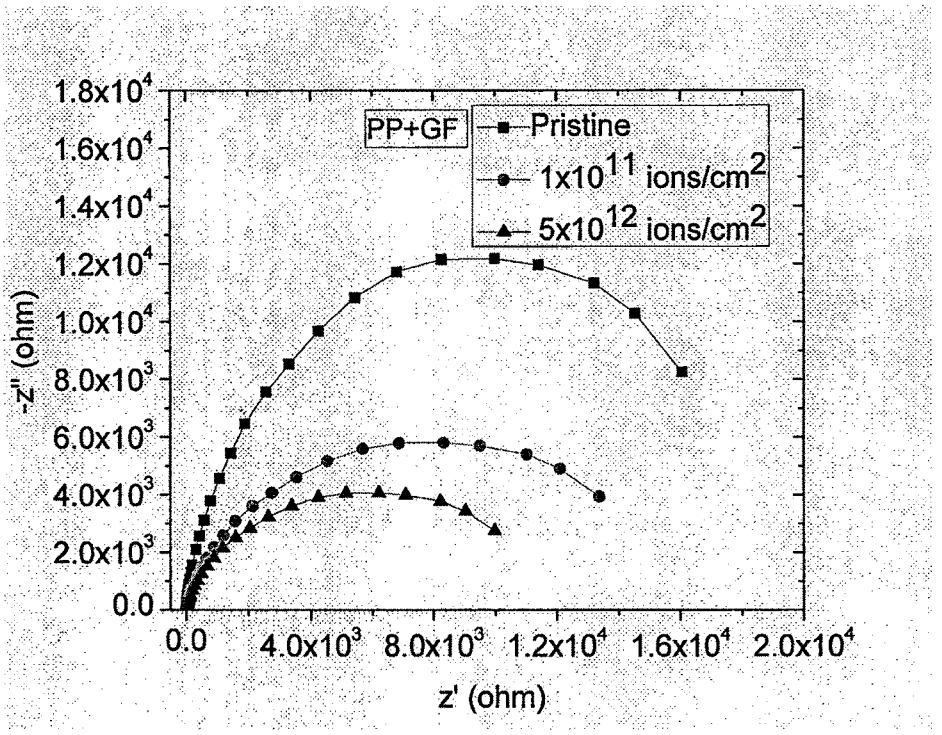

Fig. 5.13 Cole-Cole plot for pristine and irradiated PP+GF composites at different fluences.

5.2.2.4 Surface morphology

The surface morphology of pristine and irradiated PP+GF composites was measured by AFM on 5×5 μm^2 area as shown in Figure 5.14.(a,b). Each AFM image was analyzed in terms of surface average roughness (Ra). It is observed that after irradiation the roughness of the surface decreases from 58.3 nm (pristine) to 32.8 nm (irradiated $5x10^{12}$ ions/cm^2) and the surface becomes significantly smoother. This relative smoothness is probably due to the defect enhanced surface diffusion.

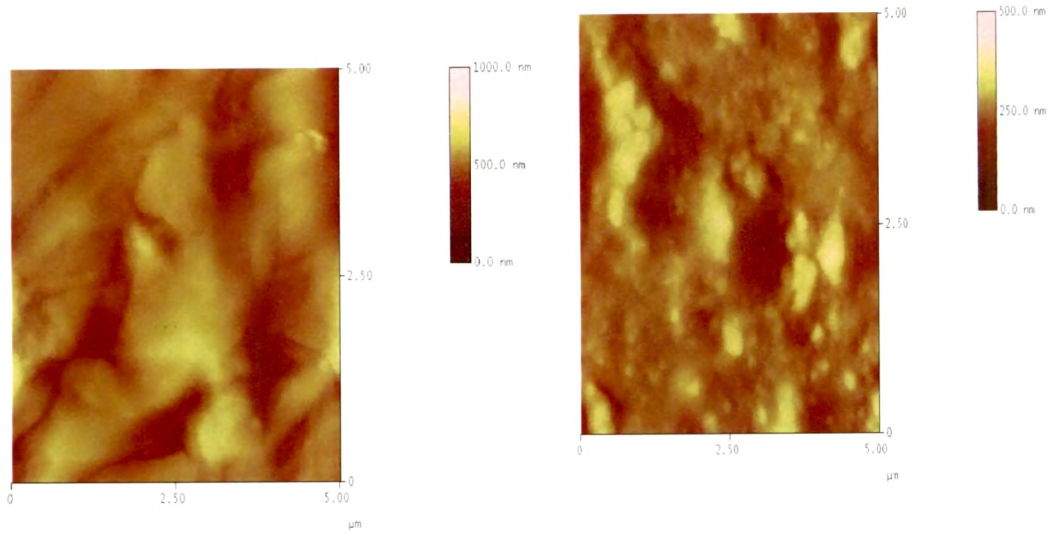

(a) (b)

Fig.5.14 AFM images of (a) pristine PP+GF composite (b) irradiated (at the fluence of $5x10^{12}$ ions/cm^2) PP+GF composite.

5.2.2.5 Conclusions

In the present study, electrical, structural, optical and surface properties of PP+GF composite were investigated and the following conclusions can be drawn.

[1] The electrical conductivity increases with increasing fluence of ion beam.

[2] The dielectric constant and dielectric loss are observed to change significantly with ion fluence. The increase in dielectric constant upon irradiation may be attributed to the disordering of the material by means of chain scission in polymer composites and as a result the increase in the number of free radicals, unsaturation etc.

[3] It is also observed that dielectric constant obeys Universal law of dielectric response at high frequencies.

[4] It is observed that optical absorption increases upon irradiation and this absorption shifted from UV–Vis to visible region for irradiated polymer composites, which

indicates the decrease in direct and indirect band gap upon ion irradiation due to formation of defects and clusters in material.

[5] From XRD results, it reveals the amorphisation of the materials upon ion beam irradiation.

[6] The surface roughness of composite decreases upon irradiation as observed from AFM studies.

5.3 Effect of Effect of 140 MeV Ag^{11+} ion irradiation on HDPE /carbon black composites

5.3.1 Introduction

High density polyethylene (HDPE) is one of the most widely used materials for the production of insulator, spacers and also for coating conducting cable used in electric power distribution networks. In this type of application, the dielectric strength is one of the properties that must be accounted in order to check the ability of the material to withstand high electric fields [40].

Swift heavy ion (SHI) irradiation of polymers is a novel technique for the creation of active sites for physical and chemical modification of polymeric materials so as to enhance or alter the properties like dielectric, optical, structural, solubility etc [41].

The aim of this work is to investigate the change in the optical, electrical and structural properties of HDPE/ CB composites after high energy ion beam irradiation. Properties and target details of composites have been discussed in Chapter-2. All pallets were irradiated with 140 MeV Ag11+ ions at the fluences of $1x10^{11}$ and $5x10^{12}$ ions/cm^2 using Pelletron accelerator at Inter University Accelerator Centre (IUAC), New Delhi.

5.3.2 Results and discussion

5.3.2.1 UV-Vis Spectroscopy

Figure 5.15 (a) shows UV- visible absorption spectra of pristine and silver ion irradiated HDPE/CB composites in the wavelength range 190-900 nm. A shift in the absorption peak towards higher wavelength was found and indicating a decrease in energy band gap of the polymer after SHI irradiation, which gives rise to the increase in conductivity of the polymer. The shift in absorption may be produced due to the creation of free radicals or unsaturations and thus have a capability of increasing the conductivity of polymer [39].

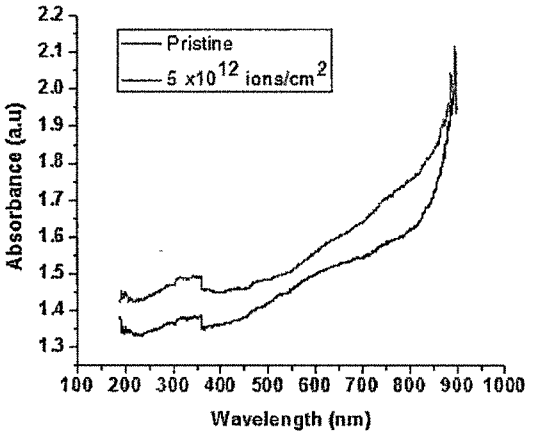

(a)

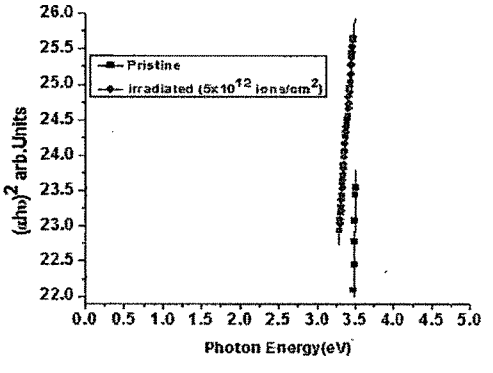

(b)

Fig. 5.15 (a) UV-Visible absorption spectra of pristine and irradiated HDPE/CB composites. (b) Plots for direct band gap (eV) in pristine and irradiated HDPE/CB composites.

From the absorption, the band gap of the polymer was calculated by linear part of Tauc's plot. The band gap was found to be 3.12 eV for pristine, and 1.71 eV for irradiated samples at the fluence of 5x 10^{12} ions/cm^2(shown in Fig5.15 (b). It may be due to the higher rate of electronic energy loss by silver ion irradiation, which affects the polymer to a greater extent [39, 21]. The calculated values of direct band gap are shown in Table 5.4.

5.3.2.2 X-ray diffraction analysis

The diffraction patterns of pristine and irradiated HDPE/CB composites are shown in figure 5.16. The three main peaks are observed at 2theta =19.52^0, 21.69^0 and 24.06^0 for the virgin sample. The nature of the peaks indicates the semi-crystalline nature of the sample. The crystallite size was calculated before and after irradiation using Scherrer's equation [23]

$b = K\lambda/L\cos\theta$

where b is FWHM in radians, λ is the wavelength of X-ray beam (1.5418Å), L is the crystallite size in Å, K is a constant which varies from 0.89 to 1.39, but for most cases it is close to 1. The degree of crystallanity (K) was calculated using the formula

K = Area under diffraction peak x 100%/ Total area under diffractogram

The average crystallite size and % crystallanity of the pristine and irradiated samples are listed in Table 5.4. Results show that crystallite size decreases slightly upon irradiation. It is also observed that the intensity of the peak decreases after irradiation,

and no significant change in the peak position is observed. This reveals that the lattice parameters do not change significantly. The decrease in intensity and broadening of the peak after irradiation indicates a decrease in crystallanity and shifted towards a disordered state. The decrease in crystallite size also observed due to irradiation [42].

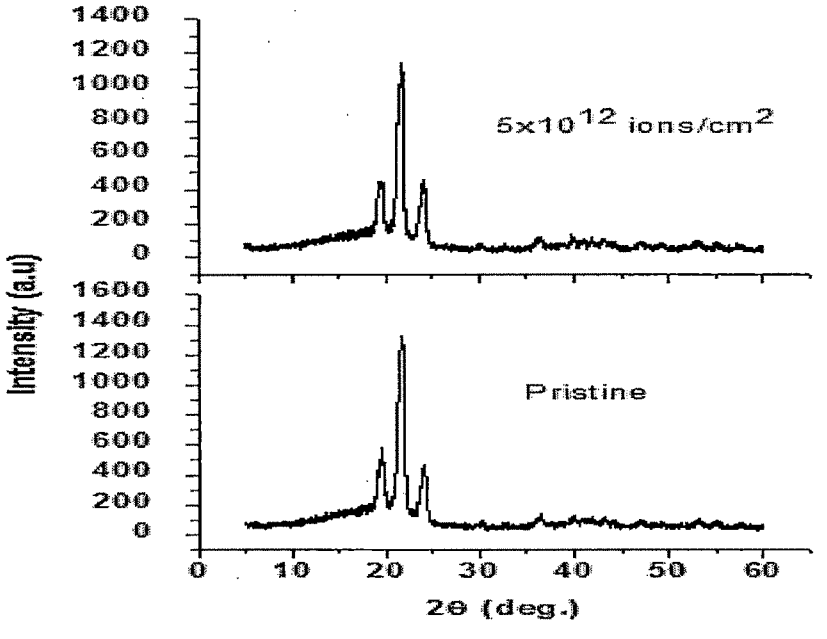

Fig.5.16 XRD patterns of pristine and irradiated HDPE/CB polymer composites at a fluence of $5x10^{12}$ ions/cm^2.

Table. 5.4

Band gap, degree of crystallinity (K) and crystalline size for HDPE/CB composites.

Samples	Band gap(eV)	Degree of Crystallinity (%)	Crystalline Size (nm)
Pristine	3.12	20.46	15.4
5 x 10^{12} ions/cm^2	1.71	19.23	14.3

5.3.2.3 Ac electrical frequency response

(a) Frequency dependence ac conductivity

AC electrical measurement was performed for pristine and irradiated samples. Figure 5.17 shows the frequency dependent electrical conductivity of pristine and irradiated composites. A sharp increase in conductivity has been observed in pristine as well as irradiated samples. It is also observed that conductivity increases as fluence increases. The increase in conductivity due to irradiation may be attributed to scissioning of the polymer chains and resulting in an increase of free redicals, unsaturation, etc. An AC filed of sufficiently high frequency may cause a net polarization, which is out of the phase with the field. This results in a.c conductivity and it appears at frequency greater than that at which traps are filled or empitted [42].

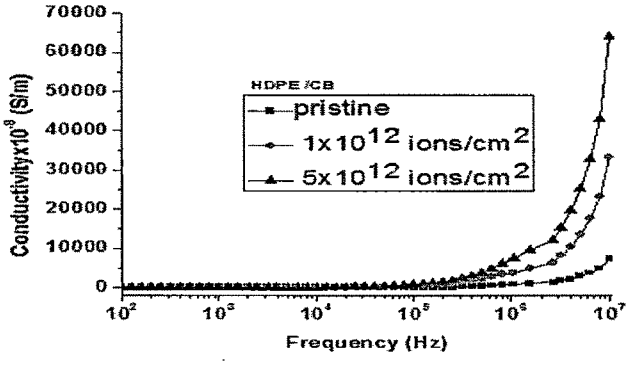

Fig.5.17 AC conductivity versus frequency for pristine and irradiated HDPE/CB composites at different fluences.

(b) Frequency dependence dielectric constant

Figure 5.18 shows the plot of dielectric constant versus frequency for pristine and irradiated HDPE/CB composites. The dielectric constant remains almost constant up to 100 kHz. At these frequencies, the motion of the free charge carriers is constant and so the dielectric constant presumably remains unchanged. As frequency increases further (i.e. beyond 100 kHz), the charge carriers migrate through the dielectric and get trapped against a defect sites and induced an opposite charge in its vicinity. At

these frequencies, the polarization of trapped and bound charges can not take place and hence the dielectric constant decreases [24]. The dielectric constant decreases at higher frequencies and obeys the Universal law [25] of dielectric response given by $\varepsilon \alpha f^{n-1}$, where n is power law exponent and varies between zero to one ($0<n<1$),and in present case n=0.32, 0.41 and 0.56 for pristine, $1x10^{11}$ ions/cm^2 and $5x10^{12}$ respectively.

According to Dissado and Hill theory at high frequency, intra-cluster motions are dominant. In intra-cluster motions, the relaxation of a dipole will produce a 'chain' response in its neighboring dipoles and the reaction of the neighboring dipoles will, in turn, affect the first dipole, so the overall effect will be seen as a single cluster dipole moment relaxation [26]. This reduces the dielectric constant at these frequencies. It is also observed that dielectric constant increases upon irradiation. The observed nature of the fluence dependence of dielectric constant in studied frequency range can be explained by the prevailing influence of the enhanced free radicals, unsaturation etc. due to the irradiation.

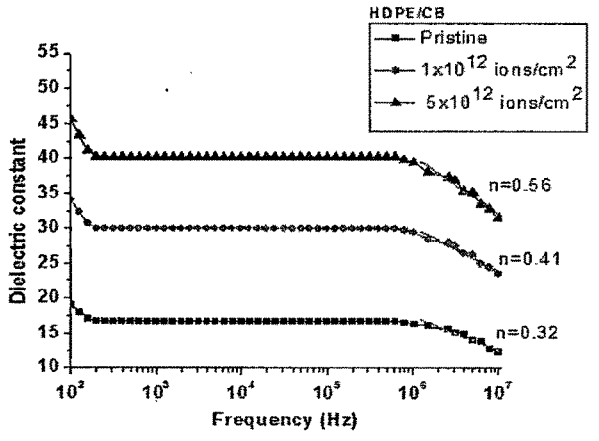

Fig. 5.18 Plot of dielectric constant versus frequency for pristine and irradiated HDPP/CB composites at different fluences.

(c) Frequency dependence dielectric loss

Figure 5.19 shows the variation of dielectric loss with frequency for pristine and irradiated samples. It is also noticed that dielectric loss increases upon irradiation. The growth in tanδ as the increase in conductivity is brought about by an increase in the conduction of residual current and the conductance of absorbance current, tanδ has positive values indicating the dominance of inductive behavior [43].

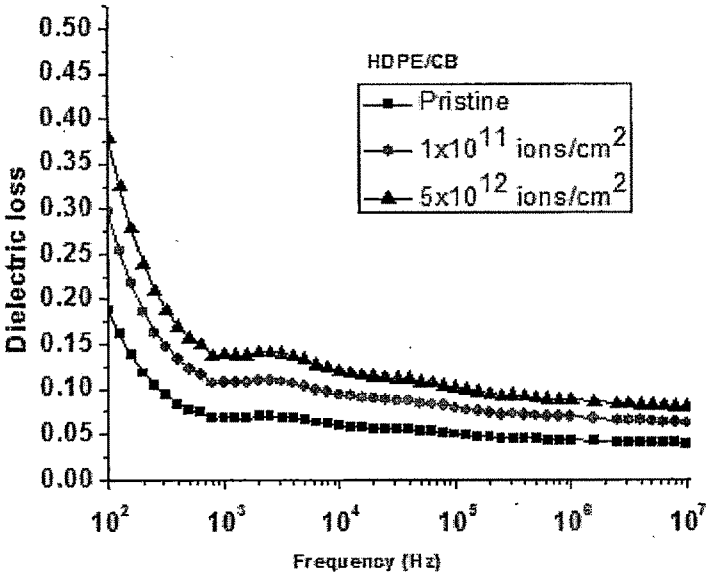

Fig. 5.19 Plot of dielectric loss versus frequency for pristine and irradiated HDPE/CB composites at different fluences.

5.3.2.4 Surface morphology of the composites

The surface morphology of pristine and irradiated HDPE/CB composites was measured by AFM on 5×5 μm^2 area as shown in Figure 5.20. Each AFM image was

analyzed in terms of surface average roughness (Ra). It is observed that after irradiation the roughness of the surface decreases from 25.3 nm (pristine) to 20.4 nm (irradiated $5x10^{12}$ ions/cm^2) and the surface became significantly smoother. This relative smoothness is probably due to defect enhanced surface diffusion.

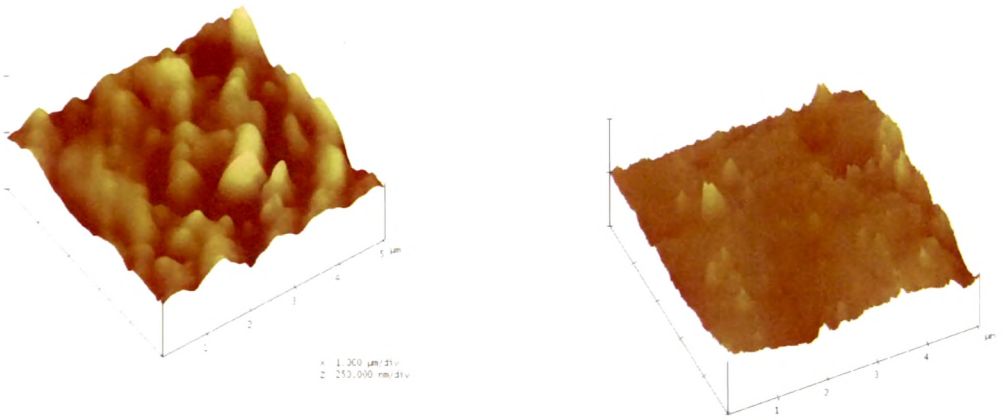

(a) **(b)**

Fig. 5.20 AFM images of (a) pristine HDPE/CB composite (b) irradiated(at the fluence of $5x10^{12}$ ions/cm^2) HDPE/CB composite.

5.3.2.5 Conclusions

The conductivity of the composites increases with an increase in frequency, and also with ion fluence. The dielectric constant and dielectric loss factor are observed to change significantly with the fluence. This reveals that the ion beam irradiation creates free radicals, unsaturation etc. due to emission of hydrogen and/or other volatile gases, which makes the polymer more conductive. It is also observed that dielectric constant obeys Universal law of dielectric response at high frequencies. It is clear from UV-visible spectra that the absorption peak is shifted towards higher wavelength and its intensity increases with ion beam irradiation, which indicates the

decrease in band gap and increase in carrier concentration. From the XRD studies, it was observed that crystalline size and crystallanity (%) of the composites are decreased due to ion irradiation, which is attributed to amorphisation of the materials. The surface roughness of composite decreases upon irradiation as observed from AFM studies

5.4 Summary

Three different composites have been studied using 140 MeV Ag^{+11} beam irradiation. AC electrical, optical, structural properties and surface morphology have been studied using different characterization techniques. Conductivity is observed to increase after irradiation in each case. The dielectric properties of composite are greatly enhanced by ion beam irradiation for all three composites systems. Thus irradiation makes the polymer more conductive. This might be attributed to breakage of chemical bonds and resulted in an increase of free radicals, unsaturation etc. It is also observed that dielectric constant obeys Universal law of dielectric response at high frequencies.

The UV-Vis spectroscopy studied shows that the absorption peak shifted towards higher wavelength, indicating a decrease in energy band gap of the composites after SHI irradiation, this gives rise to the increase in conductivity of polymer in all cases. From XRD, analysis it is observed that the crystyllinity increases on increasings the ion fluence in case of PP/TiO_2 but in case of other two composites (PP/GF and HDPE/CB) show amrophisation upon irradiation, surface morphology was studied by means AFM, which reveals that the average surface roughness increases after irradiation in case of PP+TiO_2 composites. This might be attributed to large sputtering effect due to high energy ion interaction with composite surface. In the case of other two composites PP/GF and HDPE/CB, the average surface roughness decreases upon irradiation. The decrease in surface roughness after irradiation might be attributed to defect enhanced surface diffusion.

The swift heavy ion irradiation of polymer composites reveals significant alteration in electrical, optical and structural properties of polymer composites in a controlled manner.

References

[1] E.H. Lee, Nucl. Instr. and Meth. B 151 (1999) 29.

[2] S. Bauffard, B. Gervais, C. Leray, Nucl. Instr. and Meth. B 105 (1995)

[3] A. Qureshi, D. Singh, N.L. Singh, S. Ataoglu, Arif .N. Gulluoglu, A. Tripathi, D.K. Avasthi, Nucl. Instr. Meth. B. 267(2009) 3456-3460.

[4] Dolly Singh, Anjum Qureshi, Chaitali Gavde, N.L.Singh, Ambuj Tripathi, D.K. Avasthi

Proceedings of the DAE Solid State Physics Symposium, Volume 54 (2009) 22.

[5] Dolly Singh, Anjum Qureshi , N.L. Singh, S. Ataoglu, Arif N. Gulluoglu, P.Kulriya, Ambuj Tripathi, D.K. Avasthi, To be published in Bull of Mat.Sci.

[6] N. L. Singh, Anita Sharma, V. Shrinet, A. K. Rakshit and D. K. Avasthi., Bull. Mat. Sci. 27 (2004) 101.

[7] C. A. Linkous, Environ. Sci. Technol. 34 (2000) 44754.

[8] A. Fujishima,T. N. Rao, D. A. Tryk, J.Photochem.Photobilo. C1 (2000) 1.

[9] P. Loebl, M. Huppertz, D. Mergel, Thin Solid Films 251 (1994) 72.

[10] I. Hayakawa,Y. Iwamoto, K. Kikuta, Sens. Actuators B 62 (2000) 55.

[11] A. Hagfeld, B. Didriksson, Sol. Energy Mat. Sci. Cells 31 (1994) 481.

[12] S. A. Carter, J. C.Scott, P. J. Brock, Appl. Phys. Lett. 31 (1997) 1145.

[13] J.Zhang, X. Ju, B.Wang, Q. Li, T. Liu,T.Hu, Synthetic Metals 118 (2001)181.

[14] W. Jiang, W. J.Weber, S.Thevuthasan, G. J. Exarhas, B. J. Bozlee,MRSInt.J.Nitride

Semicond.Res. 4sl (1999) G615.

[15] S. J. Pearton, J. C. Zolper, R. J. Shul, F. Ren, J. Appl.Phys. 86 (1998)1

[16] D. Fink Fundamentals of Ion-Irradiated Polymers, Springer, Berlin, 2004.

[17] D. L. Pavia, G. M. Lampman and G. S. Kriz Introduction to spectroscopy, Harcourt College Publishers, Philadelphia, 2001.

[18] Z. L. Mokrani, M. Fromm, R. Barillon, A. Chambaudet, M. Allab, Radiat. Measu. 36 (2003) 615.

[19] J. Tauc, R. Grigorovici and A. Vancu, Phys. Stat. Sol. 15 (1966) 627.

[20] J. G. Sole, L. E. Bausa L E and Jaque D, Introduction to optical spectroscopy of inorganic solids, John Wiley, New York, 2005.

[21] T.Sharma, S. Agrwal, S. Kumar, V. K. Mittal, P. C. Kalsi and V. K. Manchanda, J. Mater. Sci. 42 (2007) 1127.

[22] A.M.P. Hussain, A.Kumar, D.Saikia, F.Singh, D.K.Avasthi, Nucl. Instr. and Meth. B 240 (2005b) 871.

[23] Scherrer P. Gott Nachar 2 (1918) 98.

[24] A. K. Jonscher Nature 267 (1977) 673.

[25] A. K Jonscher 1983 Dielectric Relaxation in Solids (London: Chesla dielectric press)

[26] N. L. Singh, S. Shah, A. Qureshi, F. Singh, D. K. Avasthi, and V. Ganesan, Polym. Degrd. Stab 93 (2008) 1088.

[27] G. Kelemen, A. Lortz and G.Schom, J. Mater. Sci. 24 (1989) 333.

[28] W. Brandl, G. Marginean, V. Chirila, W. Warschewski, Carbon 42: (2004) 5-9.

[29] M. Akram, A. Javed, T.Z. Rizvi, Turk J. Phys. 29(2005)355-362.

[30] J. Murphy, 1984, The reinforced plastic Hand book; 2nd edition, Elsevier Science Ltd, UK.

[31] N.L. Singh, A. Qureshi, F. Singh, D.K. Avasthi, Mat. Sci. Eng. B 137(2007) 85-92.

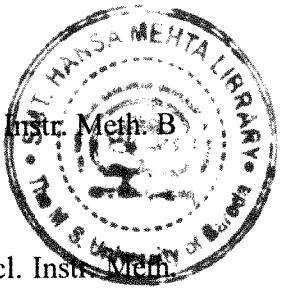

[32] N. Umeda, V.V. Bandourko, V.N. Vasilets, N. Kishimoto, Nucl. Instr. Meth. B 206(2003) 657-662.

[33] Ma. E. Martiner-Pardo, J. Cardoso, H. Vazquez, M. Agauilar, Nucl. Instr. Meth. B 140(1998) 325-340.

[34] V. M. Mohan, P. B. Bhargav, Raja, A. K. Sharma, V. V. R. Narasimha Rao,Soft Materials 5(1): (2007) 33–46.

[35] R. Kumar, Udayan. De, R. Prasad, Nucl. Instr. and Meth. B 248 (2006) 279-283.

[36] L.S. Farenza, R. M. Papaleo, A. Hallen, M.A. Araujo, R.P. Livi, B.U.R. Sundqvist, Nucl. Instr. and Meth. B 105(1995) 134-138.

[37] R.C. Ramola, S. Chandra, J. M.S. Rana, R. G. Sonkawade, P.K. Kulriya, F. Singh, D.K. Avasthi, S. Annapoorni, J.Phys. D: Appl. Phys. 41(2008) 115411

[38] M. F. Zaki, Brazilian Journal of Physics 38(2008) 558

[39] R. Mishra, S.P. Tripathy, D. Sinha, K.K. Dwivedi, S. Ghosh, D.T. Khathing, M. Muller, D. Fink, W. H. Chung, Nucl. Instrum. Meth. B 168(2000) 59.

[40] C .C. Ku, R. Liepins,1987 Dielectric Breakdown in Polymers in Electrical Properties

of Polymers-Chemical Principles (Hanser, Munich) p. 102–199.

[41] E.H.Lee. Nucl. Instrm. Methods Phys. Res. B 40(1999) 151

[42] S. Shah, N. L Singh, A. Qureshi, D. Singh, K. P. Singh, V. Shrinet, A. Tripathi, Nucl Instrm. & Methods B 266 (2008)1768.

[43] N.P.Bogoroditsky, V.V.Pasynkov, B.M.Tareev, Electrical engineering materials, Mir Publishers, Moscow (1974).